Icarus 377 (2022) 114899

Contents lists available at ScienceDirect

Icarus

journal homepage: www.elsevier.com/locate/icarus

Infrared spectra and optical constants of astronomical ices: IV. Benzene and pyridine

Reggie L. Hudson [a,*], Yukiko Y. Yarnall [a,b]

[a] Astrochemistry Laboratory, NASA Goddard Space Flight Center, Greenbelt, MD 20771, USA
[b] Universities Space Research Association, Greenbelt, MD 20771, USA

ARTICLE INFO

Keywords:
Ices
IR spectroscopy
TNOs
Titan
Organic chemistry
Infrared observations

ABSTRACT

Infrared (IR) spectra of two solid aromatic compounds, benzene (C_6H_6) and pyridine (C_5H_5N), have been recorded in their amorphous and crystalline states. Measurements of density and refractive index ($\lambda = 670$ nm) are reported for each form of each compound, quantities needed to compute IR intensities and optical constants for use in laboratory experiments and astronomical observations. These are the first such measurements of each compound's density, refractive index, and spectra at temperatures relevant to the outer solar system and interstellar medium, with all measurements being made in a single laboratory. We have used these results to determine both IR band strengths and optical constants for benzene and pyridine ices in amorphous and crystalline forms. Also, the intensity of benzene's IR absorbance near 1477 cm^{-1} is measured in samples containing H_2O-ice and compared to the strength of the same band in anhydrous amorphous benzene, the first comparison of this type for this compound. Suggestions are made for applications and future work related to the chemistry of icy bodies in the Solar System and the interstellar medium.

1. Introduction

We have reported here previously on the infrared (IR) spectra and intensities of several solid compounds of planetary and interstellar interest. Among these were ices made of acetylene C_2H_2 (Hudson et al., 2014a), ethylene C_2H_4 and ethane C_2H_6 (Hudson et al., 2014b), and most recently propyne C_3H_4, propylene C_3H_6, and propane C_3H_8 (Hudson et al., 2021). In each case we presented mid-IR spectra of amorphous and crystalline forms of each compound at cryogenic temperatures, along with band strengths and optical constants needed for quantitative work on each hydrocarbon. In a separate publication we reported similar results for methane, CH_4, the simplest common hydrocarbon (Gerakines and Hudson, 2015). Careful examination of our IR spectra enabled us to identify forbidden spectral transitions and to examine the difficulties in laboratory preparation of several forms of these icy solids.

In this paper, we continue our work on IR intensities of icy solids, while also going beyond acyclic aliphatic hydrocarbons. Here we consider benzene (C_6H_6) and pyridine (C_5H_5N), both being cyclic compounds and the latter being a heterocycle. Structures are shown in Fig. 1. The motivation for studying benzene and pyridine is straightforward, each being a prototypical aromatic compound and of interest to both interstellar and Solar System astrochemistry. Benzene's structure is one on which polycyclic aromatic hydrocarbons (PAHs) can be built, and pyridine is a simple variant, a step toward the nucleobases of DNA and RNA. Schumann et al. (2019) reported benzene in Comet 67P with the Rosetta mission's mass spectrometer, and Bézard et al. (2001) have identified benzene on both Jupiter and Saturn. Benzene is found in the interstellar medium (Cernicharo et al., 2001) and on Titan (Coustenis et al., 2003), and derivatives of both benzene and pyridine molecules have been reported in meteorites (e.g., Sephton, 2002). The enhanced stability associated with these aromatic compounds make both benzene and pyridine good candidates for detection by sample-return missions from and in situ measurements on Solar System bodies.

Benzene and pyridine ices have attracted the interest of laboratory scientists for many years. Benzene was one of the first compounds chosen by early investigations of IR intensity measurements, partly from the ease of isolating it in solid, liquid, and gaseous forms (Halford and Schaeffer, 1946; Mair and Hornig, 1949). Measurements with solid pyridine are rarer, but examples can be found (e.g., Loisel and Lorenzelli, 1967; Castellucci et al., 1969). However, what is lacking in most such work are the quantitative IR intensity results at temperatures of

* Corresponding author at: Astrochemistry Laboratory (Code 691), NASA Goddard Space Flight Center Greenbelt, MD 20771, USA.
E-mail address: reggie.hudson@nasa.gov (R.L. Hudson).

https://doi.org/10.1016/j.icarus.2022.114899
Received 29 November 2021; Received in revised form 12 January 2022; Accepted 13 January 2022
Available online 22 January 2022
0019-1035/

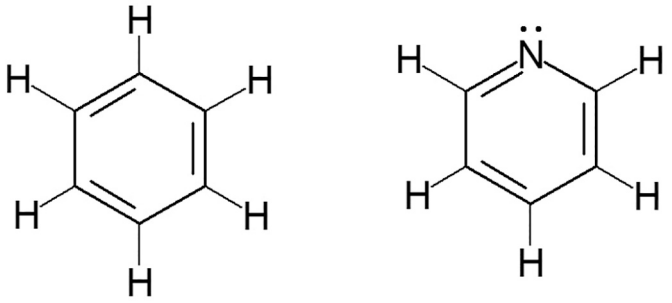

Fig. 1. Kekulé structures for benzene (left) and pyridine (right).

interest to astrochemists. Put another way, it is relatively easy to record IR spectra and document band positions, widths, and areas, but much harder to quantify such results in terms of molecular abundance or concentration.

Specific examples of the need for IR intensities and spectra of benzene and pyridine ices, and supporting values of densities and refractive indices, are readily found in the literature of observational and laboratory astrochemistry. Several recent papers of Mouzay describe the IR spectroscopy and chemistry of benzene ices at Titan (e.g., Mouzay et al., 2021), but although IR spectra are shown no details of thickness measurements are provided. In an older work, Zhou et al. (2010) claimed benzene formation by 5-keV electron irradiation of solid acetylene, but no reference spectra of benzene were shown for comparison. Those authors used $A'(1480\ \mathrm{cm^{-1}}) = 1.5 \times 10^{-18}$ cm molecule^{-1} as a benzene band strength. However, no reference for this value was supplied. Details also were lacking for how the thickness of the original ice (acetylene) was determined.

A similar situation exists regarding the need for pyridine data. Bibang et al. (2019) published a spectrum of solid pyridine at 15 K with an eye toward the chemistry in dense molecular clouds. The ice sample was stated to have a thickness of 1 μm, and presumably was amorphous, but details were lacking for how the thickness was determined. A more-recent paper from the same group (Bibang et al., 2021) showed a similar pyridine IR spectrum with the ice's thickness said to be calculated from a pyridine IR band strength. Unfortunately, no wavenumber was given for the pyridine band used, although a reference was supplied to McMurtry et al. (2016). Inspection of the latter paper revealed that the pyridine band's position was 711 cm^{-1}, but the authors failed to provide a source for the band strength.

Turning to work from our own laboratory, for our paper on benzene's radiolytic stability, we could not supply an accurate mass for the reactant ice due to the lack of density and refractive index data for benzene (Ruiterkamp et al., 2005). The same applies to our work on benzene related to meteoritic chemistry (Callahan et al., 2013) as well as to our group's study of pyridine derivatives formed by ionizing radiation (Smith et al., 2015). In each case, a more-detailed quantification of our work was hindered by a lack of information on benzene or pyridine.

Given these examples of the lack of data and traceability for benzene and pyridine IR results, here we present new work on solid forms of both compounds. We show IR spectra of both amorphous and crystalline benzene and pyridine with an emphasis on IR intensity data as opposed to the IR peak assignments and positions that have been reported repeatedly for over a half-century. Significantly, all measurements were made in our laboratory, avoiding the need to combine results from various investigators and diverse equipment. Applications can be envisioned to both Solar System objects and to the interstellar ices that contribute to comets and their chemical composition.

2. Laboratory procedures

The methods and equipment for our work with benzene and pyridine were the same as in recent papers from our laboratory (Hudson et al., 2017; Hudson et al., 2021), so only a brief description is needed. Both compounds were obtained from Sigma Aldrich (now MilliporeSigma) with stated purities of ≥99%. Each compound was used as received aside from degassing by freeze-pump-thaw cycles. One set of experiments was done with ultrapure H_2O (degassed), obtained by a reverse osmosis system, and which had a resistivity higher than 18.2 MΩ cm.

Ice samples were made by condensation of either benzene or pyridine vapor onto a KBr or CsI substrate, pre-cooled to the temperature of interest. The base temperature of our cryostat varied from about 9 to 11 K, so here we use 10 K for simplicity. The rate of deposition was such as to give an increase in an ice's thickness of a few micrometers per hour, with maximum ice thicknesses being on the order of a few micrometers. Thickness was measured using interference fringes (Hollenberg and Dows, 1961) with refractive indices determined by two-laser interferometry (Tempelmeyer and Mills, 1968), which we have found to be superior to one-laser methods, which require measurements of absolute photometric intensity. Ice densities were obtained with microbalance gravimetry, and both densities and refractive indices ($\lambda = 670$ nm) were determined under UHV conditions (~10^{-10} Torr). Deposition rates in all experiments were such as to give an increase in the resulting ice's thickness of ~1 μm hr^{-1}. See Hudson et al. (2017) for additional details.

Infrared spectra were recorded with a Thermo iS50 IR spectrometer at a resolution of 0.5 cm^{-1}, typically with 200 accumulations per spectrum. The spectral range in a few cases extended from 6500 to 400 cm^{-1}, but for the most part we focused on the 4500 to 500 cm^{-1} region. All spectra were measured in a conventional transmission mode with the IR beam perpendicular to the plane of the sample holder. Checks were made to ensure that the spectral features observed were neither resolution limited nor saturated.

Table 1
Refractive indices and densities of two aromatic compounds.[a]

	Benzene, C_6H_6		Pyridine, C_5H_5N	
Form	n	ρ/g cm^{-3}	n	ρ/g cm^{-3}
Amorphous	1.402 (10*K*)	0.769 (10 K)	1.369 (10 K)	0.781 (10 K)
Crystalline	1.620 (100*K*)	1.085 (100 K)	1.588 (130*K*)	1.149 (130 K)

[a] Values of n and ρ are averages of at least three measurements; the wavelength for n was 670 nm.

3. Results

3.1. Refractive indices and densities

A reference value for the refractive index (n) of each type of ice we studied was needed to determine ice thicknesses, which in turn were required for measuring IR band strengths and optical constants. A density (ρ) for each ice also was required for band-strength calculations. Both n and ρ proved to be difficult to find in the literature, but especially densities for amorphous ices. For example, Dawes et al. (2018) used $\rho = 0.94$ g cm^{-3} for benzene's density, citing Colson and Bernstein (1965), but inspection of the latter paper did not reveal a density value. In the case of pyridine-containing ices, Bibang et al. (2021) used $\rho = 1$ g cm^{-3}, but with no reference being given. Faced with two densities of unknown provenance, we decided that the safest course was to measure all n and ρ ourselves. Measurements of n at 670 nm, hereafter denoted n_{670}, and ρ for ices have been described in previous publications, and in principle are straightforward albeit somewhat tedious. Information is provided in Hudson et al. (2017) and, from a different laboratory, in the paper of Luna et al. (2012).

Table 1 lists the densities and refractive indices we obtained for amorphous and crystalline benzene and pyridine. Uncertainties, as standard errors, are about ±0.005 and ± 0.005 g cm^{-3} for n_{670} and ρ, respectively, in all cases. We are not aware that the density of either of the amorphous ices has been reported. Densities for crystalline benzene and crystalline pyridine, both solids being grown from liquids, have

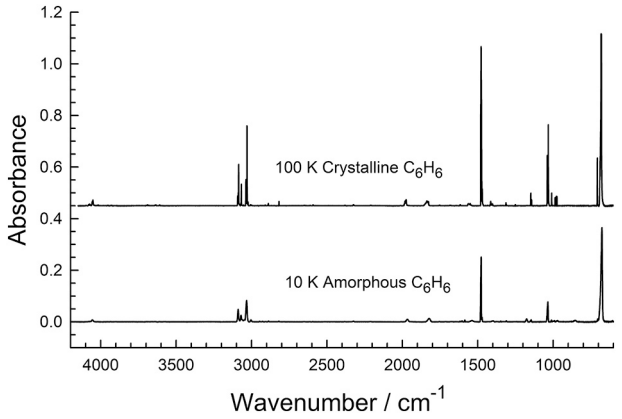

Fig. 2. Mid-IR survey spectra of amorphous and crystalline benzene (C_6H_6). Ices were grown and their spectra recorded at the temperatures indicated. The thicknesses of the amorphous and crystalline ices were about 0.96 and 0.83 μm, respectively. Spectra are offset for clarity. See the text for details.

been published in the diffraction literature, and both densities are close to what we list in Table 1 for solids formed by vapor-phase deposition. See Yarnall and Hudson (2022) for details.

3.2. Benzene - infrared spectra and intensities

The work of Ishii et al. (1996) proved valuable in the early part of our study as those authors provided information on the temperatures for making amorphous and crystalline benzene. In brief, we produced amorphous benzene ices by slow deposition of benzene vapor onto our substrate at ~10 K. Crystallization was effected by warming the resulting solid to ~60 K. However, depositing benzene vapor at 100 K gave the crystalline ice directly and faster with no additional treatment needed. Thrower et al. (2009) observed no benzene sublimation below 120 K, so all of the IR results reported here were below that temperature. As a further check, no loss of benzene was observed when a sample sat for about 16 h at 100 K. Warming crystalline benzene to about 150 K resulted in its rapid sublimation in our vacuum system.

Infrared survey spectra of amorphous and crystalline benzene are shown in Fig. 2, which agree with earlier IR results (e.g., Halford and Schaeffer, 1946; Mair and Hornig, 1949; Mouzay et al., 2021). Expansions of several regions are shown in Fig. 3. Although many aspects of these spectra are of interest, our goal was to determine spectral intensities, concentrating on the stronger features. To that end, we prepared ices of various thicknesses, recorded their IR spectra, and measured and then graphed peak heights (absorbance, $\mathscr{A}$) and band areas as a function of ice thickness (h). Eqs. (1) and (2) were the relevant guiding expressions, where ln(10) ≈ 2.303 converted absorbance to optical depth. See Hudson et al. (2021) and references therein for details.

$$\mathscr{A} = \left(\frac{\alpha'}{2.303}\right) h \tag{1}$$

$$\int_{band} (\mathscr{A})\, d\tilde{\nu} = \left(\frac{\rho_N A'}{2.303}\right) h \tag{2}$$

In Eq. (2), ρ_N is the number density (molecule cm^{-3}) of the benzene sample, calculated from our measured densities as $\rho_N = \rho\ (N_A/M)$ where M is molar mass of benzene and N_A is Avogadro's constant. All such Beer's Law plots of heights and areas as a function of ice thickness gave straight lines with slopes that led to apparent absorption coefficients (α') and band strengths (A').

Table 2 summarizes our measurements of benzene's IR intensities. It is obvious from this table that the benzene feature near 680 cm^{-1} is the strongest, with the band near 1480 cm^{-1} being somewhat weaker, and all other IR features being weaker still. Uncertainties and errors in the values we found for A' and α' are estimated to be on the order of 5% for the stronger IR features (e.g., 676 cm^{-1}), but growing to 10% for the weaker ones (e.g., 4056 cm^{-1}). See also Hudson et al. (2017) for a

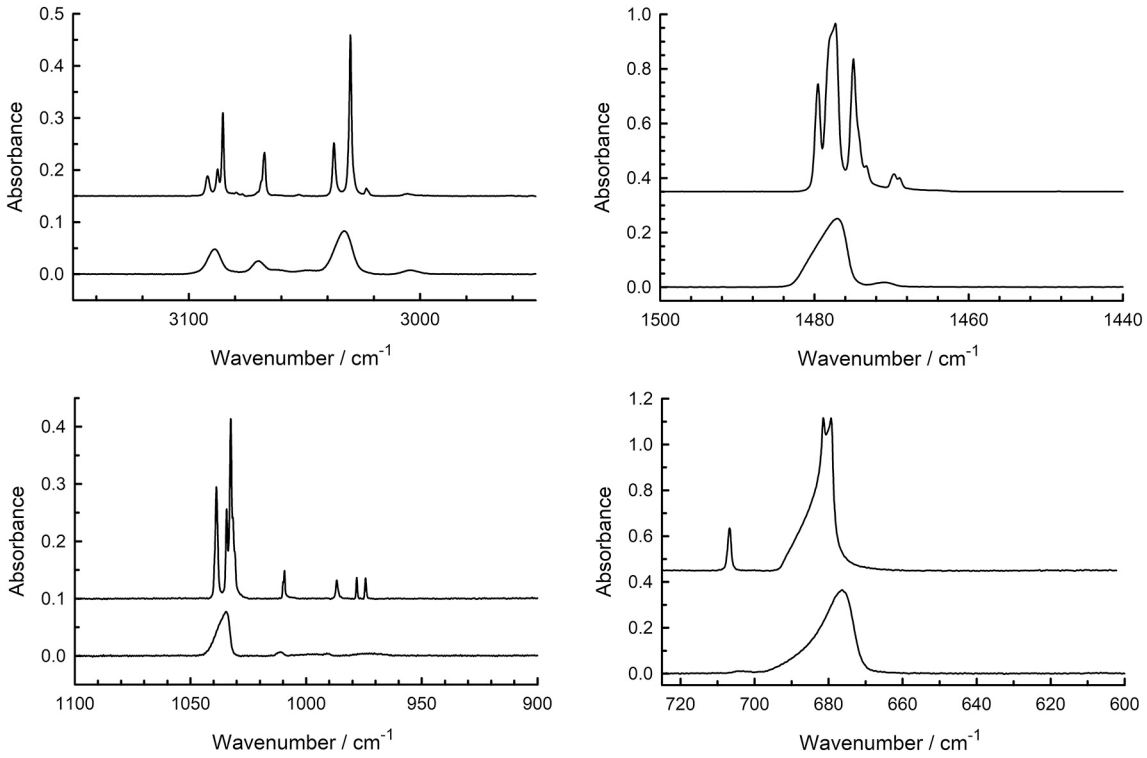

Fig. 3. Expansions of the mid-IR spectra of amorphous and crystalline benzene (C_6H_6) shown in Fig. 2. In each panel, the amorphous ice's spectrum is the lower trace and the crystalline ice's is the upper one, offset for clarity. Ices were grown and their spectra recorded at the temperatures indicated in Fig. 2.

Table 2
Positions and intensities of selected IR features of benzene ice.

Form[a]	$\tilde{\nu}$/cm^{-1}	α'/cm^{-1}	Integration range/ cm^{-1}	A'/10^{-18} cm molecule^{-1}
Amorphous	4056	148	4070–4033	0.322
	3089	1150	3110–3055	2.10
	3033	2020	3055–3016	3.25
	1477	5900	1486–1466	4.80
	1034	1760	1046–1028	1.94
	676	7920	700–666	16.2
Crystalline	4052	659	4101–4010	0.634
	3085	4790	3100–3055	2.16
	3030	9100	3055–2990	2.53
	1478	17,300	1486–1466	6.69
	1033	8190	1042–1028	2.87
	681	18,400	698–660	15.5
	679	15,100		

[a] Amorphous ice was at 10 K ($n_{670} = 1.402$, $\rho = 0.769$ g cm^{-3}) and crystalline ice was at 100 K ($n_{670} = 1.620$, $\rho = 1.085$ g cm^{-3}). See the text for variations in peak position near 681 cm^{-1} at 100 K.

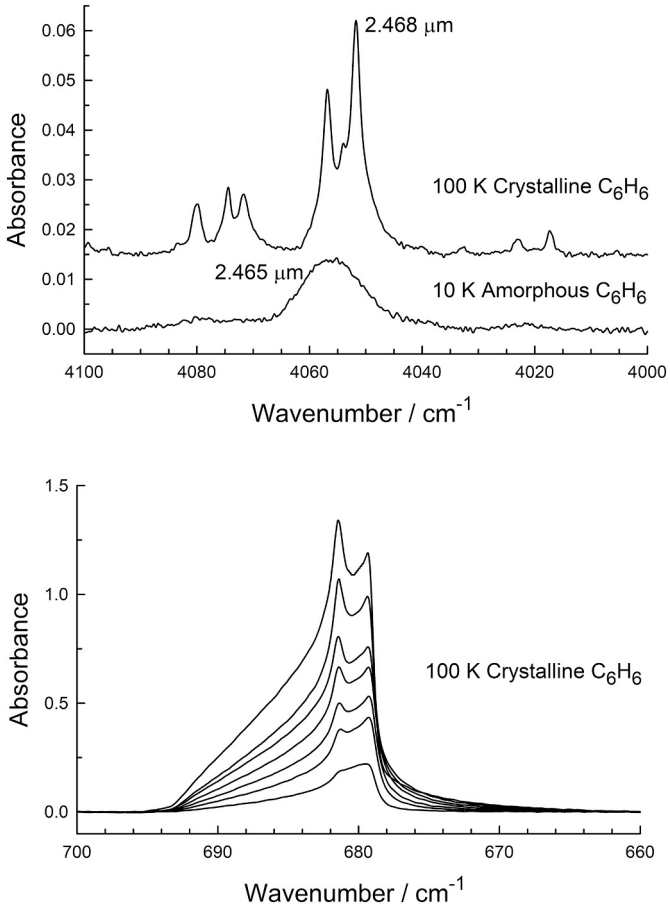

Fig. 4. Upper: Near-IR band of amorphous and crystalline benzene (C_6H_6). Ices were grown and their spectra recorded at the temperatures indicated. The thicknesses of the amorphous and crystalline ices were about 1.91 and 1.65 μm, respectively. Spectra are offset for clarity. Lower: Changes in benzene band shape with these ice thicknesses: 0.207, 0.414, 0.620, 0.827, 1.034, 1.241, and 1.654 μm.

discussion.

Two other expansions of benzene spectra are shown in Fig. 4. At the top is a feature for amorphous and crystalline benzene that might be amenable to infrared astronomical observations. Thicker ices would undoubtedly give spectra with higher signal-to-noise ratios, but the spectra in Fig. 4 certainly are enough to show the main features in this

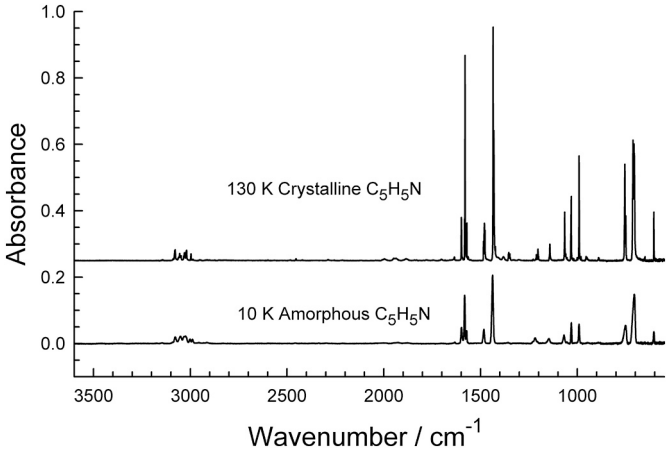

Fig. 5. Mid-IR survey spectra of amorphous and crystalline pyridine (C_5H_5N). Ices were grown and their spectra recorded at the temperatures indicated. The thicknesses of the amorphous and crystalline ices were about 0.98 and 0.84 μm, respectively. Spectra are offset for clarity. See the text for details.

region. The wavelength, in micrometers, is given for the highest peak in each trace.

The lower panel in Fig. 4 shows changes in shape of the 680-cm^{-1} band of crystalline benzene with ice thickness. No other IR feature in this compound's spectrum showed this sort of variation. We draw attention to these changes in shape as this is the IR band used to identify solid benzene on Titan (Coustenis et al., 2003; Vinatier et al., 2018). See Hudson et al. (2014a) for similar behavior with an IR band of crystalline acetylene.

Our work has focused on the IR region from about 4500 to 500 cm^{-1} as we are unaware of strong benzene features in the far-IR region of wavenumbers less than 500 cm^{-1} ($\lambda > 20$ μm). See Harada and Shimanouchi (1967) for a study of several weak far-IR bands of benzene in the 120 to 60 cm^{-1} region.

3.3. *Pyridine - infrared spectra and intensities*

Our pyridine study proceeded along the same lines followed with benzene. Ices made at 10 K had IR spectra characteristic of an amorphous solid, which crystallized rapidly on warming above 120 K. Infrared survey spectra are shown in Fig. 5, with Fig. 6 presenting expansions of selected regions. Ices were made at the temperatures indicated in Fig. 5, 10 and 130 K. (There was relatively little difference in the spectra of ices warmed from 10 to 130 K and those made by deposition at 130 K.) Crystalline ices held at 130 K for several hours showed no sublimation, but rapid sublimation did occur above 160 K.

Again, we recorded IR spectra of ices of different thicknesses, bands and peaks were measured, and Beer's law plots constructed. Tables 3 and 4 summarize our intensity results for the two forms of pyridine we examined. The IR peak near 1440 cm^{-1} is readily seen to be the most intense peak in both amorphous and crystalline pyridine.

3.4. *Optical constants*

Infrared optical constants $n(\tilde{\nu})$ and $k(\tilde{\nu})$ were calculated for our amorphous and crystalline benzene and pyridine ices using the method described by Gerakines and Hudson (2020). In brief, IR spectra were recorded of ices of different thicknesses for both forms of each compound, the baseline of each spectrum was straightened and brought to zero absorbance, if needed, and then the optical constants corresponding to each spectrum and ice thickness were calculated with an iterative Kramers-Kronig method using the measured refractive indices of Table 1. The resulting optical constants for the various thicknesses (~0.2–2 μm) of each type of ice were then averaged to give a final set,

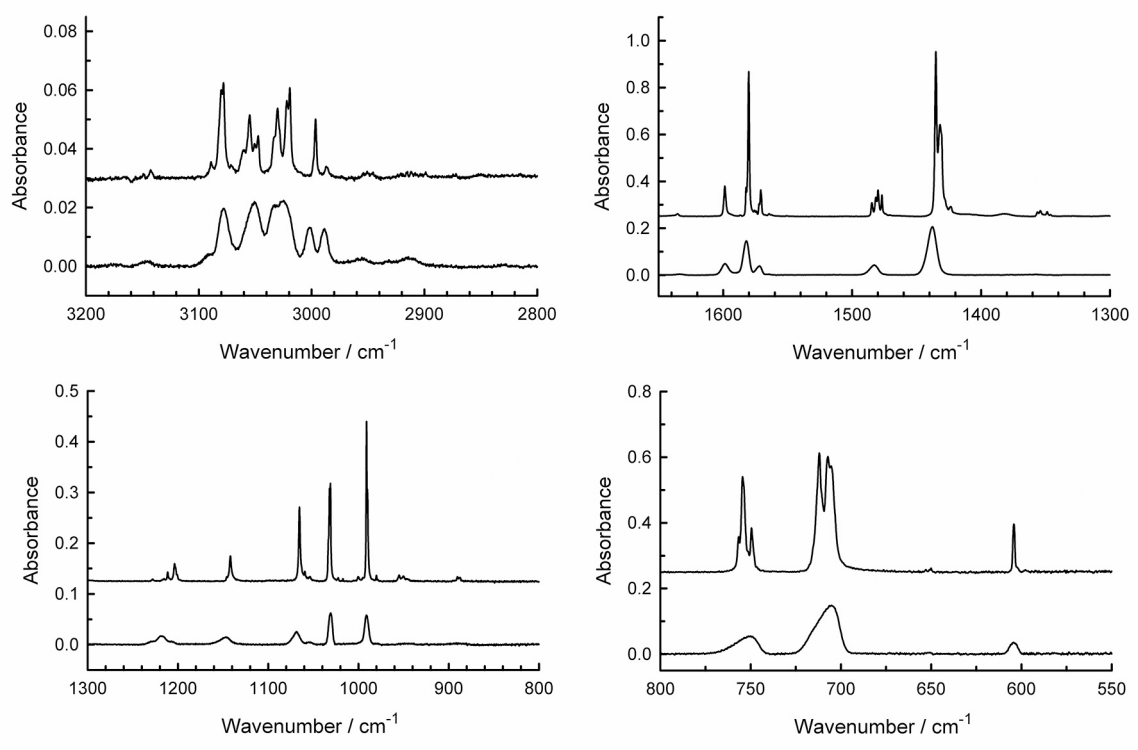

Fig. 6. Expansions of the mid-IR spectra of amorphous and crystalline pyridine (C_5H_5N) shown in Fig. 4. In each panel, the amorphous ice's spectrum is the lower trace and the crystalline ice's is the upper one, offset for clarity. Ices were grown and their spectra recorded at the temperatures indicated in Fig. 5.

Table 3
Positions and intensities of selected IR features of amorphous pyridine ices.[a]

$\tilde{\nu}$/cm^{-1}	α'/cm^{-1}	Integration range/cm^{-1}	A'/10^{-18} cm molecule^{-1}
3078	440		
3051	504		
3026	501	3110–2970	5.05
3002	289		
2989	281		
1598	1070		
1582	3370	1610–1558	5.46
1572	878		
1483	949	1500–1460	1.30
1438	4820	1460–1400	7.47
1218	361	1242–1196	1.00
1146	308	1173–1124	0.776
1068	565	1086–1040	1.11
1031	1380	1040–1025	1.19
991	1300	1007–982	1.27
750	1210	780–740	3.08
705	3350	740–690	8.84
605	748	616–599	0.691

[a] Amorphous ice was at 10 K ($n_{670} = 1.369$, $\rho = 0.781$ g cm^{-3}).

Table 4
Positions and intensities of selected IR features of crystalline pyridine ices.[a]

$\tilde{\nu}$/cm^{-1}	α'/cm^{-1}	Integration range/cm^{-1}	A'/10^{-18} cm molecule^{-1}
3078	888		
3055	573		
3030	658	3100–2970	2.772
3019	855		
2996	554		
1599	3270	1606–1588	0.878
1580	14,600	1585–1573	3.07
1571	2770	1573–1566	0.480
1480	2640	1490–1446	1.86
1435	19,980	1446–1360	10.1
1354	635	1360–1340	0.388
1142	1240	1150–1125	0.552
1065	3620	1072–1040	1.35
1031	4710	1040–1007	1.75
991	7780	997–981	1.76
754	8090	765–726	4.02
750	3220		
712	9920	726–657	11.5
707	8920		
604	3640	607–600	0.629

[a] Crystalline ice was at 130 K ($n_{670} = 1.588$, $\rho = 1.149$ g cm^{-3}).

which are shown in Figs. 7 and 8. The variation (spread) in the average values of $k(\tilde{\nu})$ was on the order of 1% for strong peaks, such as ~680 cm^{-1} for benzene and ~ 700 cm^{-1} for pyridine, rising to ~5% for weaker IR features, such as ~4056 cm^{-1} for benzene and ~ 1145 cm^{-1} for pyridine.

Our group's website has electronic versions of the same constants (https://science.gsfc.nasa.gov/691/cosmicice/constants.html). Our optical constants can be used to calculate IR spectra in either a transmission or reflection mode for ices of various thicknesses (Swanepoel, 1983; Tomlin, 1968) or can be used in numerical models for planetary, icy-satellite, and TNO surfaces. They also can be used to calculate band strengths for determining abundances from IR spectra of extraterrestrial objects.

All of our optical-constants calculations were carried out with our open-source computer routine described in Gerakines and Hudson (2020). The program is publically available in both Python and Windows-executable forms. We strongly support the development, use, and sharing of software for optical-constants and similar work, as opposed to the use of proprietary, unshared in-house software.

3.5. *Benzene in H_2O-rich ices*

The IR intensities in our tables are for neat (i.e., single-component) ices, but they also can be used to determine band strengths of benzene

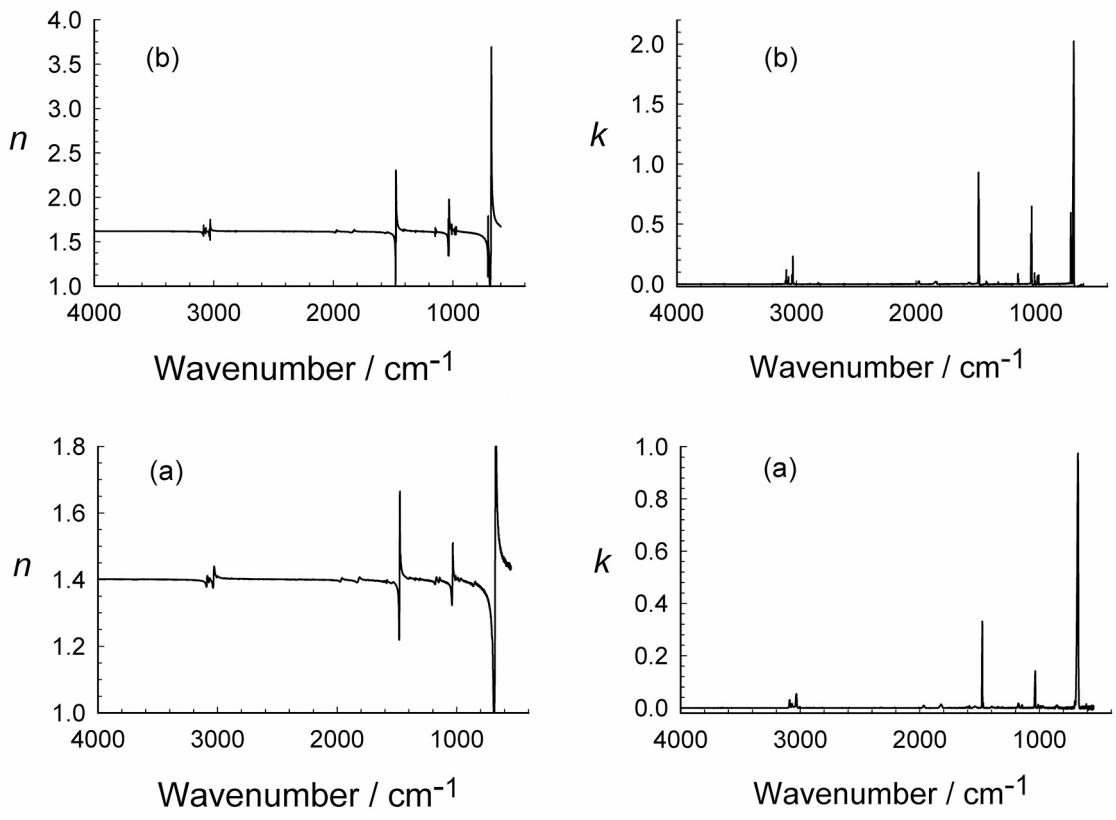

Fig. 7. Optical constants *n* and *k* for (a) amorphous and (b) crystalline benzene. Ices were grown and their IR spectra for optical-constants calculations were recorded at the temperatures indicated in Fig. 2.

or pyridine in, for example, mixtures rich in H_2O-ice. We illustrated the method in a recent paper in which we measured the intensity of the C≡N stretching vibration in the IR spectra of amorphous HCN and amorphous H_2O + HCN mixtures, finding that the literature band strength, measured indirectly, must be raised by 100% to match the value found by direct measurement. We also found that the C≡N band strength of solid HCN was essentially the same in the presence and absence of H_2O-ice. See Gerakines et al. (2022) for details.

As another illustration of this same method, we prepared and recorded IR spectra of several H_2O + C_6H_6 ices of roughly the same thickness (~1 μm), but different H_2O-to-C_6H_6 ratios, all at 10 K. A separate, dedicated deposition line was used for each compound, with the rates of deposition, and thus column density in each ice, being determined from the measurements we made separately on each reagent. Plotting the area of the benzene band near 1477 cm^{-1} in each ice mixture as a function of benzene column density gave the graph in Fig. 9, the x axis being the equivalent of the product "$\rho_N\, h$" in Eq. (2). The slope of the line in Fig. 9, after multiplication by 2.303, gave $A' = 5.22 \times 10^{-18}$ cm $molecule^{-1}$ for that IR band in H_2O-rich mixtures, slightly greater than the value in the absence of H_2O-ice, $A' = 4.80 \times 10^{-18}$ cm $molecule^{-1}$, but just within an experimental error of ~10%. The H_2O-to-C_6H_6 ratios used for the six points of Fig. 9 were 100:1, 50:1, 30:1, 20:1, 10:1, and 5:1. We note that the shape of the 1477 cm^{-1} feature of benzene (Fig. 3) becomes more symmetrical in the presence of H_2O-ice, and the peak's position shifts slightly to about 1480 cm^{-1}, changes we leave for a future study.

Our choice of benzene's 1477 cm^{-1} IR feature for study was based on its relative sharpness and absolute intensity (Fig. 2). It also is located well away from the strong IR features of silicates and solid H_2O seen in the IR spectra of interstellar ices.

4. Discussion

4.1. IR spectra and intensities

Our spectra of benzene and pyridine ices agree qualitatively with previous work in terms of peak positions and approximate relative intensities. The asymmetric band shapes seen near 1480, 1030, and 680 cm^{-1} in spectra of amorphous benzene, and near 710 cm^{-1} for amorphous pyridine, indicate inhomogeneous broadening, as also seen in the IR spectra of other ices, such as C_2H_2 and C_2H_6 (Hudson et al., 2014a; Hudson et al., 2014b). The main differences in the spectra of the amorphous and crystalline forms of both benzene and pyridine are the sharpening, splitting, and shifts in position of IR bands on crystallization, characteristic changes noted for many years by us and others (e.g., Malherbe and Bernstein, 1951; Nightingale and Wagner, 1954). Several such intensity changes on crystallization are quite dramatic, such as those near 1035 cm^{-1} for benzene and around 1580 and 1440 cm^{-1} for pyridine.

We have not found previous intensity measurements on solid pyridine with which to compare our results, but several investigations have been published for solid benzene, although only for the crystalline solid. As an example, Hollenberg and Glover (1967) published band strengths for crystalline C_6H_6 at 85 K, finding no more than about a 5% variation from 60 to 130 K. Their reported A' values are about 13% larger than ours (Table 2) for the benzene features near 1477, 1034, and 676 cm^{-1}. Part of the reason for the difference is the choices of *n* and ρ used by those authors. The fact that no integration ranges were specified hinders a more precise comparison. Qualitatively, our amorphous-pyridine spectrum resembles that of Bibang et al. (2019) and our crystalline-pyridine spectrum resembles that of Castellucci et al. (1969). The latter authors described, but did not show, the spectrum of amorphous pyridine. The peak positions they reported agree with those we

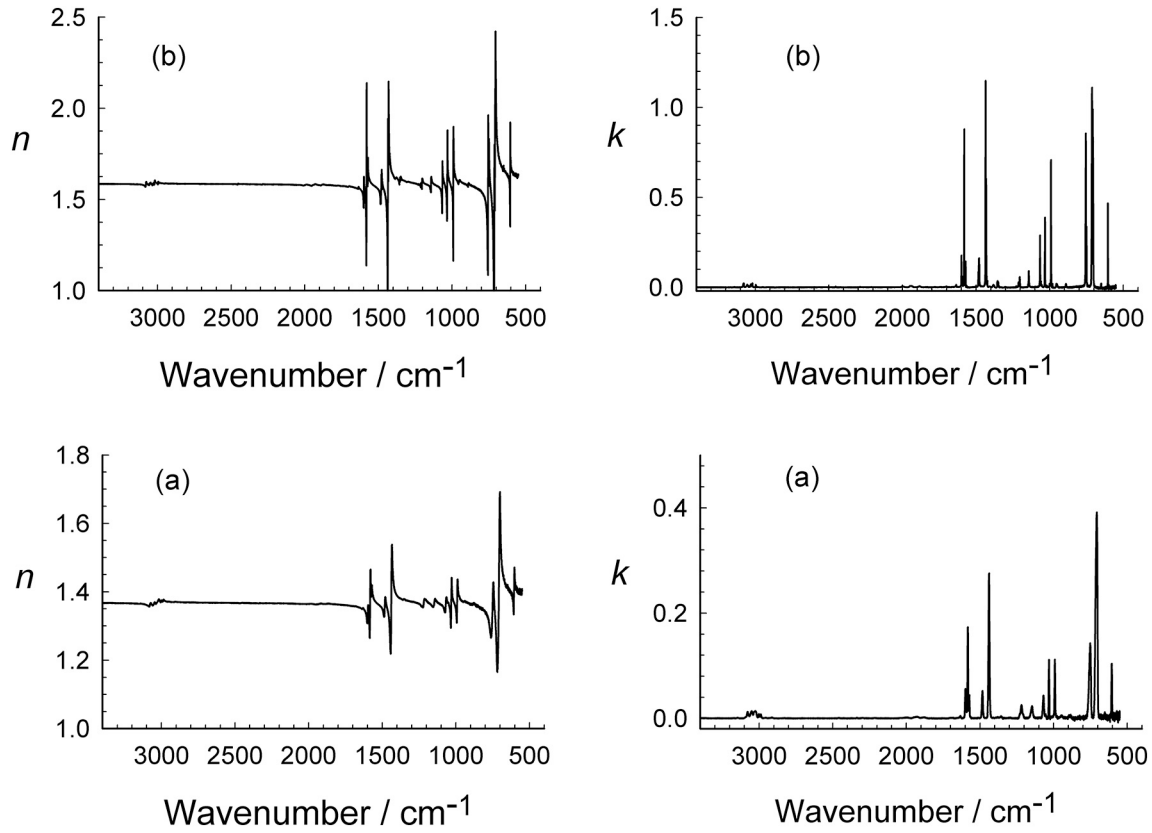

Fig. 8. Optical constants *n* and *k* for (a) amorphous and (b) crystalline pyridine. Ices were grown and their IR spectra for optical-constants calculations were recorded at the temperatures indicated in Fig. 5.

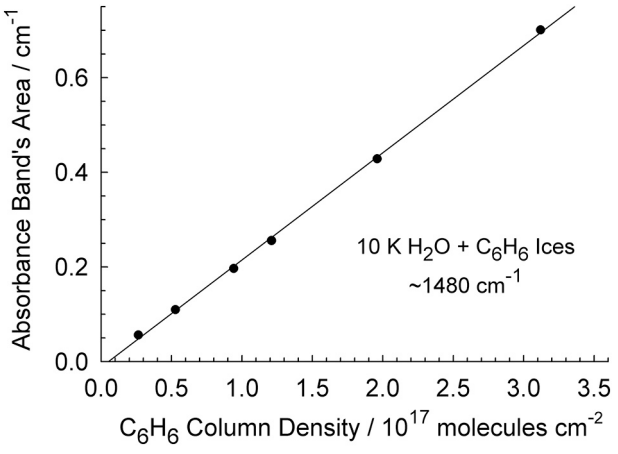

Fig. 9. The area of the C_6H_6 IR band at ~1480 cm^{-1} in six H_2O + C_6H_6 ices having H_2O:C_6H_6 ratios of 100:1, 50:1, 30:1, 20:1, 10:1 and 5:1 (lower left to upper right). Each ice was grown and its spectrum recorded at 10 K.

observed.

A less obvious way to compare our results to earlier work involves liquid-phase spectra of benzene and pyridine. To the extent that amorphous solids can be described as frozen liquids, as opposed to crystalline materials, then there should be a good match between our spectra of amorphous ices and their liquid-phase counterparts. From the literature of a century ago, we find that the room-temperature IR results of benzene and pyridine from Coblentz (1905) indeed agree qualitatively with the 10-K amorphous ice spectra in our figures. Similarly, there is good agreement for peak positions and relative intensities between IR spectra of our amorphous ices and the liquid-phase spectra in the Sigma Aldrich atlas (Pouchert, 1997) and in the NIST Chemistry WebBook (http://webbook.nist.gov/chemistry/).

In a separate publication we compared our crystalline benzene and crystalline pyridine densities, measured by microbalance gravimetry, to results from diffraction work finding differences on the order of 2% (Yarnall and Hudson, 2022). As for refractive indices, our 1.402 for amorphous C_6H_6 is close to the 1.42 ± 0.07 of Stubbing et al. (2020), and our 1.620 is near those authors' value of 1.63 ± 0.08 for crystalline benzene. We have not found refractive indices for solid pyridine in the literature.

We also have not located refereed, published optical constants for frozen benzene and pyridine. We stress that optical constants depend directly on the reference refractive indices used, corresponding to our measured values for ices in Table 1. Our experience with our λ = 670 nm results on amorphous and crystalline solids is that *n*(amorphous) < *n* (crystalline), so that we do not recommend adopting a single value of *n* for calculating optical constants of both types of ice. The use of a questionable refractive index, one from a liquid, or one from a different form or phase than one is studying, introduces an error that propagates through the resulting calculations and which no amount of computation or spectroscopic care can remove.

4.2. *Some applications and extensions*

Applications of our results cover both laboratory and observational astrochemistry. With robust band strengths, optical constants, densities, and refractive indices in hand, laboratory IR work with benzene and pyridine ices should be increasingly accurate. Examples from our own lab would be increased accuracy in measuring rates of either formation or destruction of benzene and pyridine by radiolysis or photolysis. Also, if intensities of IR features are needed beyond those we have reported then they can be found quickly by simple scaling of the intensities in our

tables. We have found studies in the literature, some already cited, that involve extensive tabulations of reaction yields, rate constants, and cross sections, but with the underlying spectroscopic or other quantities either poorly known or never measured. Such studies can acquire an unsupported veneer of numerical precision, and should be used with caution if quantitative results are needed.

We also again mention our measurements with H_2O-ice. Our finding that the presence of H_2O-ice changes A'(~1477 cm^{-1}) for benzene by only ~8% should give a degree of comfort and confidence in the application of our work to multi-component mixtures. We have now applied our method to both a polar (HCN) and a non-polar (C_6H_6) molecule in H_2O-rich ices, and band strengths have been found to undergo only small changes. It remains to be seen if these two compounds and our chosen conditions are anomalies or if they are part of a general behavior for a variety of situations. Experiments with other molecular combinations and temperatures are needed.

Our work here has focused on the difficult task of IR intensity measurements. With our results in hand, it should now be easier to correlate absorbance peak positions and band widths with concentration changes over a range of ice temperatures. Measurements of thicker ices could improve on the intensity measurement of the near-IR results we found for benzene at 4056 cm^{-1} ($\lambda \sim 2.47$ μm). The method we used to measure a band strength for $H_2O + C_6H_6$ mixtures can easily be extended to H_2O-rich mixtures of pyridine and other compounds. We fully expect that H_2O or other ices will produce reasonably symmetrical IR features for amorphous benzene and pyridine ices, and will remove thickness-dependent splittings, such as we have presented for crystalline benzene. Such changes remain to be documented.

The obvious connection to observational work comes through IR spectra of extraterrestrial objects. Within the Solar System, benzene already has been reported on Titan (Coustenis et al., 2003) based on the IR band near 680 cm^{-1} that we measured. Our quantification of this feature, through measurements at a higher resolution than other studies, should be of value. The closest thing to a near-IR band in our benzene results probably is the small feature near 4056 cm^{-1} ($\lambda \sim 2.47$ μm), for which Table 2 lists intensities. As for pyridine, although IR detections have not yet been reported, its strong peaks in the 700 cm^{-1} region, particularly for the crystalline ice, could be useful as they are further removed, compared to benzene, from the large absorbance of H_2O-ice around 800 cm^{-1}.

As a final future application of our results, 134 K appears to be the lowest temperature at which the vapor pressure of crystalline benzene has been measured (Dubois et al., 2021). We have been unable to find any published results for vapor pressures of pyridine ices (but see Geraghty et al., 1984). With the method of Khanna et al. (1990), the IR band strengths we have reported here can be used for lower-temperature measurements for benzene and new measurements for pyridine.

Declaration of Competing Interest

None.

Acknowledgments

NASA funding through the Cassini Data Analysis Program is acknowledged, as is support from NASA's Planetary Science Division Internal Scientist Funding Program through the Fundamental Laboratory Research (FLaRe) work package at the NASA Goddard Space Flight Center. Assistance also was provided through the Goddard Center for Astrobiology and the NASA Astrobiology Institute. YYY thanks the NASA Postdoctoral Program for her fellowship. Perry Gerakines (NASA), Marla Moore (NASA, retired), Robert Ferrante (US Naval Academy), and Mark Loeffler (Northern Arizona University) contributed to various stages of this work. Two anonymous reviewers are also thanked for helpful comments.

References

Bézard, B., Drossart, P., Encrenaz, T., Feuchtgrube, H., 2001. Benzene on the giant planets. Icarus 154, 492–500.
Bibang, P.C.J.A., Agnihotri, A.N., Augé, B., et al., 2019. Ion radiation in icy space environments: synthesis and radioresistance of complex organic molecules. Low Temp. Phys. 45, 590–597.
Bibang, P.C.J.A., Agnihotri, A.N., Boduch, P., et al., 2021. Radiolysis of pyridine in solid water. Eur. Phys. J. D. 45, 57.
Callahan, M.P., Gerakines, P.A., Martin, M.G., Peeters, Z., Hudson, R.L., 2013. Icarus 226, 1201–1209.
Castellucci, E., Shrana, G., Verderame, F.D., 1969. Infrared spectra of crystalline and matrix isolated pyridine and pyridine-d_5. J. Chem. Phys. 51, 3762–3770.
Cernicharo, J., Heras, A.M., Tielens, A.G.G.M., Pardo, J.R., et al., 2001. Infrared space Observatory's discovery of C_4H_2, C_6H_2, and benzene in CRL 618. Astrophys. J. 546, L123–L126.
Coblentz, W.W., 1905. Investigations of Infra-Red Spectra. Carnegie Institution of Washington, Washington, DC.
Colson, S.D., Bernstein, E.R., 1965. First and second triplets of solid benzene. J. Chem. Phys. 43, 2661–2669.
Coustenis, A., Salama, A., Schulz, B., Ott, S., Lellouch, E., et al., 2003. Titan's atmosphere from ISO mid-infrared spectroscopy. Icarus 161, 383–403.
Dawes, A., Pascual, N., Mason, N.J., Gärtner, S., Hoffmann, S.V., Jones, N.C., 2018. Probing the interaction between solid benzene and water using vacuum ultraviolet and infrared spectroscopy. Phys. Chem. Chem. Phys. 20, 15273–15287.
Dubois, D., Iraci, L.T., Barth, E.L., Salama, F., Vinatier, S., Sciamma-O'Brien, E., 2021. Investigating the condensation of benzene (C_6H_6) in Titan's south polar cloud system with a combination of laboratory, observational, and modeling tools. Planet. Sci. J. 2, 1 (15 pages).
Geraghty, P., Wixom, M., Francis, A.H., 1984. Photocalorimetric spectroscopy and ac calorimetry of thin surface films. J. Appl. Phys. 55, 2780–2785.
Gerakines, P.A., Hudson, R.L., 2015. The infrared spectra and optical constants of elusive amorphous methane. Astrophys. J. 805, L20–L24.
Gerakines, P.A., Hudson, R.L., 2020. A modified algorithm and open-source computational package for the determination of infrared optical constants relevant to astrophysics. Astrophys. J. 901, 1 (10 pages).
Gerakines, P.A., Yarnall, Y.Y., Hudson, R.L., 2022. Direct measurements of infrared intensities of HCN and H_2O + HCN ices for laboratory and observational astrochemistry. MNRAS 509, 3515–3522. https://doi.org/10.1093/mnras/stab2992. In press.
Halford, R.S., Schaeffer, O.A., 1946. Motion of molecules in condensed phases. II. The infrared spectra of benzene solid, liquid, and vapor in the range from 3 to 16.7 μ. J. Chem. Phys. 14, 141–149.
Harada, I., Shimanouchi, T., 1967. Far-infrared spectra of crystalline benzene at 138 K and intermolecular forces. J. Chem. Phys. 46, 2708–2714.
Hollenberg, J.L., Dows, D.A., 1961. Measurement of absolute infrared absorption intensities in crystals. J. Chem. Phys. 34, 1061–1063.
Hollenberg, J.L., Glover, D.E., 1967. Infrared reflection spectrum of thin-film solid benzene. J. Phys. Chem. 71, 1544–1546.
Hudson, R.L., Ferrante, R.F., Moore, M.H., 2014a. Infrared spectra and optical constants of astronomical ices: I. Amorphous and crystalline acetylene. Icarus 228, 276–287.
Hudson, R.L., Gerakines, P.A., Moore, M.H., 2014b. Infrared spectra and optical constants of astronomical ices: II. Ethane and ethylene. Icarus 243, 147–148.
Hudson, R.L., Loeffler, M.J., Gerakines, P.A., 2017. Infrared spectra and band strengths of amorphous and crystalline N_2O. J. Chem. Phys. 146, 0243304.
Hudson, R.L., Yarnall, Y.Y., Gerakines, P.A., Coones, R.T., 2021. Infrared spectra and optical constants of astronomical ices: III. Propane, propylene, and propyne. Icarus 354, 114033 (10 pages).
Ishii, K., Nakayama, H., Yoshida, T., Usui, H., Koyama, K., 1996. Amorphous state of vacuum-deposited benzene and its crystallization. Bull. Chem. Soc. Jpn. 69, 2831–2838.
Khanna, R.K., Allen Jr., J.E., Masterton, C.M., Zhao, G., 1990. Thin-film infrared spectroscopic method for low-temperature vapor pressure measurements. J. Phys. Chem. 94, 440–444.
Loisel, J., Lorenzelli, V., 1967. IR spectra of crystallized pyridine at liquid nitrogen temperatures. J. Mol. Struct. 1, 157–171.
Luna, R., Satorre, M.Á., Domingo, M., Millán, C., Santonja, C., 2012. Density and refractive index of binary CH_4, N_2 and CO_2 ice mixtures. Icarus 221, 186–191.
Mair, R.D., Hornig, D.F., 1949. The vibrational spectra of molecules and complex ions in crystals. II. Benzene. J. Chem. Phys. 17, 1236–1247.
Malherbe, F.E., Bernstein, H.J., 1951. Infrared spectra of rapidly solidified vapors. J. Chem. Phys. 19, 1607–1608.
McMurtry, B.M., Turner, A.M., Saito, S.E.J., Kaiser, R.I., 2016. On the formation of niacin (vitamin B3) and pyridine carboxylic acids in interstellar model ices. Chem. Phys. 472, 173–184.
Mouzay, J., Couturier-Tamburelli, I., Piétri, N., Chiavassa, T., 2021. Experimental simulation of Titan's stratospheric photochemistry: benzene (C_6H_6) ices. J. Geophys. Res. - Planets 126, 1–18.
Nightingale, R.E., Wagner, E.L., 1954. The vibrational spectra and structure of solid hydroxylamine and deutero-hydroxylamine. J. Chem. Phys. 22, 203–208.
Pouchert, C., 1997. Aldrich Library of FT-IR Spectra, 2nd edition.
Ruiterkamp, R., Peeters, Z., Moore, M.H., Ehrenfreund, P., 2005. A quantitative study of proton irradiation and UV photolysis of benzene in interstellar environments. Astron. Astrophys. 440, 391–402.

Schumann, M., Altwegg, K., Balsiger, H., et al., 2019. Aliphatic and aromatic hydrocarbons in comet 67P/Churyumov-Gerasimenko seen by ROSINA. Astron. Astrophys. 630, 1–11.
Sephton, M.A., 2002. Organic compounds in carbonaceous meteorites. Nat. Prod. Rep. 19, 292–311.
Smith, K.E., Gerakines, P.A., Callahan, M.P., 2015. Metabolic precursors in astrophysical ice analogs: implications for meteorites and comets. Chem. Commun. 51, 11787–11790.
Stubbing, J.W., McCoustra, M.R.S., Brown, W.A., 2020. A new technique for determining the refractive index of ices at cryogenic temperatures. Phys. Chem. Chem. Phys. 22, 25353–25365.
Swanepoel, R., 1983. Determination of the thickness and optical constants of amorphous silicon. J. Phys. E: Sci. Instrum. 16, 1214–1222.
Tempelmeyer, K.E., Mills, D.W., 1968. Refractive index of carbon dioxide cryodeposit. J. Appl. Phys. 39, 2968–2969.
Thrower, J.D., Collings, M.P., Rutten, F.J.M., McCoustra, M.R.S., 2009. Laboratory investigations of the interaction between benzene and bare silicate grain surfaces. MNRAS 394, 1510–1518.
Tomlin, S.G., 1968. Optical transmission and reflection formulae for thin films. Brit. J. Appl. Phys. (J. Phys. D) 2, 1667–1671.
Vinatier, S., Schmitt, B., Bézard, B., Rannou, P., et al., 2018. Study of Titan's fall southern stratospheric polar cloud composition with Cassini/CIRS: detection of benzene ice. Icarus 310, 89–104.
Yarnall, Y.Y., Hudson, R.L., 2022. Crystalline ices – densities and comparisons for planetary and interstellar applications. Icarus 373, 1–2. https://doi.org/10.1016/j.icarus.2021.114799.
Zhou, L., Zheng, W., Kaiser, R.I., Landera, A., Mebel, A.M., Liang, M., Yung, Y., 2010. Cosmic-ray mediated formation of benzene on the surface of Saturn's moon titan. Astrophys. J. 718, 1243–1251.